Inorg. Chem. **2007**, *46*, 2328–2338

Ruthenium Nitrosyls Derived from Polypyridine Ligands with Carboxamide or Imine Nitrogen Donor(s): Isoelectronic Complexes with Different NO Photolability

Michael J. Rose,[†] Apurba K. Patra,[†] Eric A. Alcid,[†] Marylin M. Olmstead,[‡] and Pradip K. Mascharak*,[†]

Department of Chemistry and Biochemistry, University of California, Santa Cruz, California 95064, and Department of Chemistry, University of California, Davis, California 95616

Received November 2, 2006

As part of our search for photoactive ruthenium nitrosyls, a set of $\{RuNO\}^6$ nitrosyls has been synthesized and structurally characterized. In this set, the first nitrosyl $[(SBPy_3)Ru(NO)](BF_4)_3$ (**1**) is derived from a polypyridine Schiff base ligand $SBPy_3$, while the remaining three nitrosyls are derived from analogous polypyridine ligands containing either one ($[(PaPy_3)Ru(NO)](BF_4)_2$ (**2**)) or two ($[(Py_3P)Ru(NO)]BF_4$ (**3**) and $[(Py_3P)Ru(NO)(Cl)]$ (**4**)) carboxamide group(s). The coordination structures of **1** and **2** are very similar except that in **2**, a carboxamido nitrogen is coordinated to the ruthenium center in place of an imine nitrogen in case of **1**. In **3** and **4**, the ruthenium center is coordinated to two carboxamido nitrogens in the equatorial plane and the bound NO is trans to a pyridine nitrogen (in **3**) and chloride (in **4**), respectively. Complexes **1**–**3** contain N6 donor set, and the NO stretching frequencies (ν_{NO}) correlate well with the N–O bond distances. All four diamagnetic $\{RuNO\}^6$ nitrosyls are photoactive and release NO rapidly upon illumination with low-intensity (5–10 mW) UV light. Interestingly, photolysis of **1** generates the diamagnetic Ru(II) photoproduct $[(SBPy_3)Ru(MeCN)]^{2+}$ while **2**–**4** afford paramagnetic Ru(III) species in MeCN solution. The quantum yield values of NO release under UV illumination ($\lambda_{max} = 302$ nm) lie in the range 0.06–0.17. Complexes **3** and **4** also exhibit considerable photoactivity under visible light. The efficiency of NO release increases in the order **2** < **3** < **4**, indicating that photorelease of NO is facilitated by (a) the increase in the number of coordinated carboxamido nitrogen(s) and (b) the presence of negatively charged ligands (like chloride) trans to the bound NO.

Introduction

Nitric oxide (NO) has been recognized as an important signaling molecule that plays key roles in several biological processes including vasodilation, neurotransmission, and immune response.[1−6] NO is synthesized endogenously by nitric oxide synthase (NOS) and is normally present in the cell at nanomolar levels. At such concentrations, NO regulates certain proteins such as soluble guanylate cyclase (sGC)[1] which controls cellular cyclic guanylate monophosphate (cGMP) levels and maintains blood pressure.[2] The production of NO at high concentrations by macrophages is thought to be critical for host defense against infection.[4] NO also induces apoptosis in cancer cells at high concentrations[5] possibly via inhibition of cellular respiration.[6] NO has also been implicated in limiting tumor metastasis,[5] suggesting NO may be a potent anticancer agent. These findings have prompted extensive research activity in the area of developing NO donors as therapeutic agents and as tools in biological research.

* To whom correspondence should be addressed. E-mail: pradip@chemistry.ucsc.edu.
[†] University of California, Santa Cruz.
[‡] University of California, Davis.

(1) (a) Ignarro, L. J. *Nitric Oxide: Biology and Pathobiology*; Academic Press: San Diego, 2000. (b) Feelisch, M.; Stamler, J. S., Editors. *Nitric Oxide Research*; John Wiley and Sons: Chichester, UK, 1996. (c) Fukuto, J. M.; Wink, D. A. *Met. Ions Biol. Syst.* **1999**, *36*, 547.
(2) Lincoln, J.; Burnstock, G. *Nitric Oxide in Health and Disease*; Cambridge University Press: New York, 1997.
(3) (a) Kalsner, S., Ed. *Nitric Oxide Free Radicals in Peripheral Neurotransmission*; Birkhauser: Boston, 2000.
(4) Ko, G. Y.; Fang, F. C. *Nitric Oxide and Infection*; Kluwer Academic/Plenum Publishers: New York, 1999.
(5) (a) Xie, K.; Huang, S. *Free Radical Biol. Med.* **2003**, *34*, 969. (b) Xie, K.; Wang, B.; Shi, Q.; Abbruzzese, J. L.; Qinghua, X.; Le, X. *Int. J. Gastrointest. Cancer* **2001**, *29*, 25. (c) Lala, P. K.; Orucevic, A. *Cancer Metastasis Rev.* **1998**, *17*, 91.
(6) (a) Boyd, C. S.; Cadenas, E. *J. Biol. Chem.* **2002**, *383*, 411. (b) Cooper, C. E. *Trends Biochem. Sci.* **2002**, *27*, 33. (c) Brown, G. C. *Biochim. Biophys. Acta* **2001**, *1504*, 46.

10.1021/ic0620945 CCC: $37.00
Published on Web 02/22/2007

A variety of organic compounds such as nitrites (e.g., trinitroglycerol), nitrosothiols (e.g., *S*-nitrosopenicillamine, SNAP), and diazeniumdiolates (commonly known as NONOates) have been used clinically as vasodilators.[7−10] Some metal-based NO donors have also been used to deliver NO.[11] For example, the iron−nitrosyl sodium nitroprusside ($[Fe(NO)(CN)_5]^{2-}$, SNP) is used in hypertensive episodes.[7] Unfortunately, release of NO from these systemic NO donors is dependent on enzymatic reactions, heat, or pH, and hence, target specificity is mostly precluded. Release of auxiliary ligands from metal-based NO donors like SNP also leads to deleterious side effects.[12] In contrast, compounds that release NO strictly upon exposure to light could provide a more selective means of NO delivery. Ruthenium nitrosyls (NO complexes) are particularly attractive in this regard because they are thermally stable yet release NO when exposed to UV light. For example, complexes such as $[Ru(salen)(Cl)(NO)]$,[13] $[Ru(NH_3)_4(NO)X](BF_4)_3$ (X = isonicotinamide, pyrazine)[14] and $[Ru(NO)(pyS_4)](Tos)$ (Tos = tosylate)[15] all release NO when irradiated with UV light (200 W Hg/Xe lamp). More detailed investigation on the photolability of NO from these $\{RuNO\}^6$ complexes[16] has identified several factors that influence the efficiency of NO release. For example, Franco and co-workers explored the effects of various ligands **L** in the series $[(NH_3)_4Ru(NO)(\mathbf{L})]^{3+}$ and found that inclusion of strong σ-donors like phosphites (such as $P(OEt)_3$) substantially increased the efficiency of NO release over ligands like pyridine.[17] Ford and co-workers have shown that in the series $[(salen)Ru(NO)(\mathbf{L})]^{0/+}$, charged ligands like Cl^- accelerated the release of NO compared to neutral ligands like water.[18]

In our efforts toward syntheses of photoactive ruthenium nitrosyls, we have previously reported a thermally stable $\{RuNO\}^6$ nitrosyl, namely $[(PaPy_3)Ru(NO)](BF_4)_2$, that releases NO upon exposure to low-intensity (5 mW) UV light.[19] This water-soluble ruthenium nitrosyl is derived from the pentadentate polypyridine ligand $PaPy_3H$ ($PaPy_3H$ = *N*,*N*-bis(2-pyridylmethyl)amine-*N*-ethyl-2-pyridine-2-carboxamide; H = dissociable proton) that contains a single carboxamide group in the ligand framework. $[(PaPy_3)Ru(NO)](BF_4)_2$ is an efficient NO donor and has been used to deliver NO to several biological targets including myoglobin and cyctochrome *c* oxidase.[19,20a] We have also reported a set of photoactive $\{RuNO\}^6$ nitrosyls derived from tetradentate pyridine-based planar dicarboxamide N4 ligands that rapidly releases NO upon UV illumination.[21] The NO photolability of these $\{RuNO\}^6$ nitrosyls raised questions regarding the role(s) of the carboxamido N donor(s) in labilizing the Ru−NO bond. We have therefore investigated the photoactivity of $\{RuNO\}^6$ nitrosyls derived from polypyridine ligands containing 0, 1, and 2 carboxamide groups. The structures of these designed ligands are shown below. These pentadentate ligands are structurally similar to each other and are expected to afford $\{RuNO\}^6$ nitrosyls with similar structural features. The syntheses of these ligands

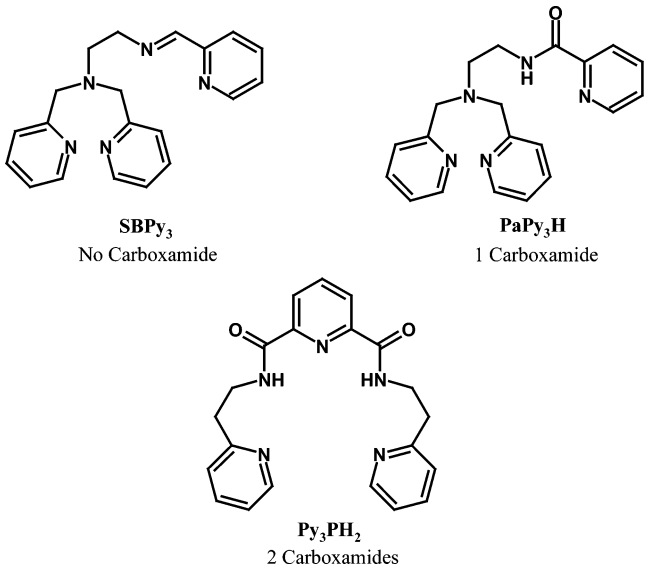

and selected metal complexes (metal = Fe, Mn, or Co) have already been reported by us.[22−28] In this paper, we report

(7) (a) Wang, P. G.; Cai, T. B.; Taniguchi, N. *Nitric Oxide Donors: for Pharmaceutical and Biological Applications*; Wiley-VCH: Weinheim. 2005.
(8) (a) Hrabie, J. A.; Keefer, L. K. *Chem. Rev.* **2002**, *102*, 1135. (b) Keefer, L. K.; Nims, R. W.; Davies, K. M.; Wink, D. A. *Methods Enzymol.* **1996**, *268*, 281.
(9) (a) Janero, D. R.; Bryan, N. S.; Saijo, F.; Dhawan, V.; Schwalb, D. J.; Warren, M. C.; Feelisch, M. *Proc. Natl. Acd. Sci. U.S.A.* **2004**, *101*, 16958. (b) Rassaf, T.; Feelisch, M.; Kelm, M. *Free Radical Biol. Med.* **2004**, *36*, 413.
(10) Butler, A. R.; Megson, I. L. *Chem. Rev.* **2002**, *102*, 1155.
(11) Ford, P. C.; Bourassa, J.; Miranda, K.; Lee, B.; Lorkovic, I.; Boggs, S.; Kudo, S.; Laverman, L. *Coord. Chem. Rev.* **1998**, *171*, 185.
(12) (a) Alaniz, C.; Watts, B. *Ann. Pharamcother.* **2005**, *39*, 388. (b) Venugopal, A.; Topf, J. M. *Am. J. Kidney Dis.* **2006**, *168*, A60.
(13) (a) Works, C. F.; Ford, P. C. *J. Am. Chem. Soc.* **2000**, *122*, 7592. (b) Bordini, J.; Hughes, D. L.; da Motto Neto, J. D.; da Cunha, C. J. *Inorg. Chem.* **2002**, *41*, 5410.
(14) Gomes, M. G.; Davanzo, C. U.; Silva, S. C.; Lopes, L. G. F.; Santos, P. S.; Franco, D. W. *J. Chem. Soc., Dalton Trans.* **1998**, 601.
(15) (a) Sellmann, D.; Engl, K.; Heinemann, F. W. *Eur. J. Inorg. Chem.* **2000**, 423. (b) Sellmann, D.; Häussinger, D.; Gottschalk-Gaudig, T.; Heinemann, F. W. *Z. Naturforsch.* **2000**, *55b*, 723.
(16) The $\{M-NO\}^n$ notation used in this paper is that of Feltham and Enemark. See Enemark, J. H.; Feltham, R. D. *Coord. Chem. Rev.* **1974**, *13*, 339.
(17) Carlos, R. M.; Ferro, A. A.; Silva, H.; Gomes, M. G.; Borges, S.; Ford, P. C.; Tfouni, E.; Franco, D. W. *Inorg. Chim. Acta.* **2004**, *357*, 1381.
(18) Works, C. F.; Jocher, C. J.; Bart, G. D.; Bu, X.; Ford, P. C. *Inorg. Chem.* **2002**, *41*, 3728.
(19) Patra, A. K.; Olmstead, M. M; Mascharak, P. K. *Inorg. Chem.* **2003**, *42*, 7363.
(20) (a) Szundi, I.; Rose, M. J.; Sen, I.; Eroy-Reveles, A. A.; Mascharak, P. K.; Einarsdottir, O. *Photochem. Photobiol.* **2006**, *82*, 1377. (b) Eroy-Reveles, A. A.; Leung, Y.; Mascharak, P. K. *J. Am. Chem. Soc.* **2006**, *128*, 7166.
(21) Patra, A. K.; Rose, M. J.; Murphy, K. M.; Olmstead, M. M.; Mascharak, P. K. *Inorg. Chem.* **2004**, *43*, 4487.
(22) Patra, A. K.; Olmstead, M. M.; Mascharak, P. K. *Inorg. Chem.* **2002**, *41*, 5403.
(23) Rowland, J. M.; Olmstead, M. M.; Mascharak, P. K. *Inorg. Chem.* **2001**, *40*, 2810.
(24) (a) Patra, A. K.; Afshar, R.; Olmstead, M. M.; Mascharak, P. K. *Angew. Chem. Intl. Ed.* **2002**, *41*, 2512. (b) Patra, A. K.; Rowland, J. M.; Marlin, D. S.; Bill, E.; Olmstead, M. M.; Mascharak, P. K. *Inorg. Chem.* **2003**, *42*, 6812.
(25) (a) Ghosh, K.; Eroy-Reveles, A. A.; Avila, B.; Holman, T. R.; Olmstead, M. M.; Mascharak, P. K. *Inorg. Chem.* **2004**, *43*, 2988. (b) Ghosh, K.; Eroy-Reveles, A. A.; Olmstead, M. M.; Mascharak, P. K. *Inorg. Chem.* **2005**, *44*, 8469.
(26) Afshar, R. K.; Bhalla, R.; Rowland, J. M.; Olmstead, M. M.; Mascharak, P. K. *Inorg. Chim. Acta* **2006**, *359*, 4105.

the syntheses, structures, and photochemical behaviors of $[(SBPy_3)Ru(NO)](BF_4)_3$ (**1**, where $SBPy_3$ = *N*,*N*-bis(2-pyridylmethyl)amine-*N*-ethyl-2-pyridine-2-aldimine), $[(PaPy_3)Ru(NO)](BF_4)_2$ (**2**), and $[(Py_3P)Ru(NO)]BF_4$ (**3**, where Py_3PH_2 = *N*,*N*-bis(2-(2-pyridyl)ethyl)pyridine-2,6-dicarboxamide; H = dissociable protons), as well as a detailed comparison of the efficiency of photorelease of NO from these $\{RuNO\}^6$ nitrosyls on the basis of their spectroscopic, photochemical, and electrochemical properties.

Experimental Section

Materials and Reagents. Commercially available $RuCl_3 \cdot xH_2O$ from Sigma-Aldrich was used to prepare the starting salts $RuCl_3 \cdot 3H_2O$,[21] $[Ru(DMSO)_4Cl_2]$,[29] and $[Ru(MeCN)_4Cl_2]$,[30] according to their published procedures. $AgBF_4$ was obtained from Alfa Aesar, and all other reagents were procured from Aldrich Chemical Co. The solvents were purified according to standard procedures: EtOH and MeOH were distilled from Mg/I_2; MeCN and CH_2Cl_2 from CaH_2; Et_2O, THF, and toluene from Na; DMF and DMSO from BaO. The ligands $SBPy_3$,[22] $PaPy_3H$,[23] and Py_3PH_2,[27] were synthesized as previously described. The complex $[(PaPy_3)Ru(Cl)]BF_4$ (**6**) was synthesized according to the published report.[19] NO gas was supplied by Spectra Gases, Inc. and purified as previously described.[21]

Syntheses of Compounds. $[(SBPy_3)Ru(NO)](BF_4)_3$ (1). A batch of 0.219 g (0.453 mmol) of $[Ru(DMSO)_4Cl_2]$ was heated to reflux in 5 mL of EtOH to generate a bright orange solution. Separately, 0.150 g (0.453 mmol) of $SBPy_3$ ligand was dissolved in 5 mL of EtOH and added to the hot solution of $[Ru(DMSO)_4Cl_2]$. The resulting orange-red solution was heated to reflux for 30 min. At this point, 0.069 g (1.0 mmol) of solid $NaNO_2$ was added to the reaction mixture, and the heating was continued for another 30 min. Next, a dilute solution of $HBF_4 \cdot Et_2O$ (0.322 g, 2.0 mmol) in 5 mL of EtOH was slowly added to the refluxing reaction. The light brown solid that separated from the hot solution was collected by filtration under N_2 and washed several times with dry Et_2O. The crude product was extracted with MeCN and loaded onto a silica gel column equilibrated with MeCN + 1% HBF_4 and eluted with MeCN with increasing amounts (0.1% to 1%) of HBF_4. The orange fraction that eluted with MeCN containing 0.5% HBF_4 was collected, and the solvent was removed to isolate the desired product. Yield: 110 mg (34%). Orange needles suitable for X-ray diffraction were grown via diffusion of CH_2Cl_2 into a MeCN solution of the complex. Anal. Calcd for $C_{20}H_{21}B_3F_{12}N_6ORu$ (**1**): C, 33.23; H, 2.93; N, 11.63; Found: C, 33.19; H, 2.98; N, 11.66. Selected IR frequencies (KBr disk, cm^{-1}): 1920 (vs, ν_{NO}), 1635 (w), 1611 (m, ν_{CN}), 1482 (w), 1453 (m), 1306 (w), 1221 (w), 1083 (s), 1034 (vs), 769 (m), 533 (w), 521 (w). Electronic spectrum in MeCN, λ_{max} in nm (ϵ in M^{-1} cm^{-1}): 253 (10 910), 315 (6060), 468 (440). ^1H NMR in CD_3CN, δ from TMS: 9.17 (d 1H), 8.92 (s 1H), 8.66 (t 1H), 8.57 (d 1H), 8.31 (m 3H), 7.93 (d 2H), 7.62 (m 4H), 5.42 (dd 4H), 4.00 (m 4H).

$[(PaPy_3)Ru(NO)](BF_4)_2$ (2). Method A. A batch of 0.100 g of $[(PaPy_3)Ru(Cl)]BF_4$ (0.176 mmol) was dissolved in 10 mL of MeOH and heated to reflux to obtain a clear brick red solution. A slurry of $AgBF_4$ (0.034 g, 0.176 mmol) in 2 mL of MeOH was added to this hot solution. The reaction was heated for 4 h when a turbid orange solution was obtained. The solution was cooled to room temperature and filtered through a Celite pad. The filtrate was degassed and then again heated to reflux temperature. A slow stream of NO gas was passed through the hot solution for 45 min. The reaction mixture was finally cooled to −20 °C when an orange solid was precipitated. The solid was collected by filtration and washed several times with Et_2O. This procedure afforded pure **2** as judged by its IR, ^1H NMR, and electronic spectra. Yield: 45 mg (40%).

Method B. A slurry of 0.209 g (0.432 mmol) of $[Ru(DMSO)_4Cl_2]$ was heated to reflux in 3 mL of EtOH to obtain a clear yellow solution. Separately, 0.011 g (0.475 mmol) of NaH was dissolved in 3 mL of EtOH and mixed with 0.150 g (0.432 mmol) of $PaPy_3H$. The solution of the deprotonated ligand was then added directly to the hot solution of $[Ru(DMSO)_4Cl_2]$, which immediately became deep red. After 3 h of heating at reflux temperature, a batch of 0.033 g of solid $NaNO_2$ (0.475 mmol) was added, and the heating was continued for 2 h. Next, a dilute solution of $HBF_4 \cdot Et_2O$ in 3 mL of EtOH was added to the hot reaction mixture. Complex **2** precipitated from the solution as an orange solid within a few minutes. The orange solid was collected by filtration of the hot solution and washed several times with dry Et_2O. The crude product was extracted with 10 mL of MeCN and filtered to remove NaCl. Finally, the solvent was removed in vacuo to isolate pure **2** in 26% yield.

$[(Py_3P)Ru(NO)]BF_4$ (3). A slurry of 0.150 g (0.278 mmol) of $[(Py_3P)Ru(NO)(Cl)]$ (see below) was taken in 50 mL of warm DMF and treated with 1 equiv of $AgBF_4$ (0.054 g, 0.278 mmol) dissolved in 5 mL of DMF. The orange solution was briefly heated to 80 °C when a turbid solution was obtained. Upon cooling to room temperature, the reaction mixture was filtered through Celite and the solvent removed in vacuo. The residue was triturated several times with MeCN to remove residual DMF. Next, the orange solid was stirred in 8 mL of THF for 1 h to remove a trace of impurity and finally the solid was collected by filtration. Yield: 120 mg (79%). Red needles suitable for X-ray diffraction were grown via diffusion of Et_2O vapor into a solution of the complex in MeCN. Anal. Calcd for $C_{23}H_{23}BF_4N_6O_3Ru$ (**3**): C, 44.60; H, 3.74; N, 13.57; Found: C, 44.68; H, 3.76; N, 13.72. Selected IR frequencies (KBr disk, cm^{-1}): 1877 (vs, ν_{NO}), 1646 (s), 1611 (vs, ν_{CO}), 1481 (w), 1441 (w), 1370 (m), 1084 (m), 775 (m), 679 (w). Electronic spectrum in MeCN, λ_{max} in nm (ϵ in M^{-1} cm^{-1}): 260 (18 100), 530 sh (400). ^1H NMR in CD_3CN, δ from TMS: 9.08 (d 1H), 8.43 (t 1H), 8.19 (t 2H), 8.14 (t 1H), 7.94 (d 1H), 7.88 (t 1H), 7.67 (m 2H), 7.44 (d 1H), 7.27 (t 1H), 4.59 (m 2H), 3.95 (dd 1 H), 3.34 (t 1H), 3.27 (m 1H), 3.15 (dd 1H), 2.82 (m 1H), 2.57 (m 1H).

$[(Py_3P)Ru(NO)(Cl)]$ (4). A batch of 0.200 g of Py_3PH_2 (0.535 mmol) was dissolved in 30 mL of EtOH and treated with 0.028 g of NaH (1.07 mmol) in 5 mL of EtOH. The resulting pale yellow solution was degassed by freeze−pump−thaw technique, and 1 equiv of $[Ru(MeCN)_4Cl_2]$ (0.178 g, 0.535 mmol) was added to the frozen solution. Upon warming to room temperature under N_2, a deep orange-red solution was obtained. This solution was then heated to reflux for 2 h. Next, a batch of 0.040 g of solid $NaNO_2$ (0.585 mmol) was added to the hot solution under N_2 and the heating was continued for 1 h. The deep red solution was then cooled to room temperature and filtered. A degassed solution of $HBF_4 \cdot Et_2O$ (300 μL, 1.065 mmol) in 5 mL of EtOH was then slowly added (via a cannula) to the reaction mixture kept at 0 °C. The resulting precipitate was collected under N_2, extracted with 20 mL of MeCN, and loaded onto a silica gel column equilibrated

(27) (a) Chavez, F. A.; Olmstead, M. M.; Mascharak, P. K. *Inorg. Chem.* **1996**, *35*, 1410. (b) Chavez, F. A.; Rowland, J. M.; Olmstead, M. M.; Mascharak, P. K. *J. Am. Chem. Soc.* **1998**, *120*, 9015.
(28) Marlin, D. S.; Olmstead, M. M.; Mascharak, P. K. *Inorg. Chem.* **1999**, *38*, 3258.
(29) Evans, I. P.; Spencer, A.; Wilkinson, G. *J. Chem. Soc. Dalton Trans.* **1973**, 204.
(30) Newton, W. E.; Searless, J. E. *Inorg. Chim. Acta* **1973**, *7*, 349.

with CH_2Cl_2 containing 5% MeOH. It was then eluted with CH_2Cl_2 with increasing amounts of MeOH (5%-20%). An orange band was eluted with CH_2Cl_2 containing 15% MeOH. Diffusion of Et_2O into this orange fraction afforded 60 mg of [$(Py_3P)Ru(NO)(Cl)$] as orange-red microcrystals. Yield: 25%. X-ray quality crystals of red plates were grown via diffusion of Et_2O into a dilute solution of the complex in MeCN. Anal. Calcd for $C_{23}H_{23}ClN_6O_3Ru$ (**4**): C, 48.64; H, 4.08; N, 14.80; Found: C, 48.49; H, 4.15; N, 14.78. Selected IR frequencies (KBr disk, cm^{-1}): 1862 (vs, ν_{NO}), 1621 (s, ν_{CO}), 1602 (vs, ν_{CO}), 1479 (w), 1443 (w), 1381 (m), 1091 (w), 767 (m), 679 (w). Electronic spectrum in MeCN, λ_{max} in nm (ϵ in M^{-1} cm^{-1}): 260 (17 500), 510 sh (330). ^1H NMR in $(CD_3)_2SO$, δ from TMS: 9.14 (d 1H), 8.55 (d 1H), 8.47 (t 1H), 8.24 (t 1H), 8.24 (t 1H), 8.05 (m 2H), 7.88 (d 1H), 7.78 (t 1H), 7.72 (t 1H), 7.35 (d 1H), 7.23 (t 1H), 4.33 (m 1H), 4.10 (m 1H), 3.89 (m 1H), 3.61 (dd 1H), 3.37 (m 1H), 3.17 (m 1H), 3.12 (m 1H), 3.07 (dd 1H).

[$(Py_3P)Ru(Cl)$]·MeCN (5·MeCN). A batch of 0.200 g of $RuCl_3 \cdot 3H_2O$ (0.763 mmol) was dissolved in 30 mL of EtOH and heated to reflux for 3 h to generate a green solution. The solvent was then removed in vacuo, and the residue was dissolved in 5 mL of DMF. Separately, a batch of 0.286 g of Py_3PH_2 (0.763 mmol) was dissolved in 5 mL of DMF and added to slurry of 0.042 g of NaH (1.679 mmol) in 5 mL of DMF. The solution of the deprotonated ligand thus generated was then added to the green ruthenium solution and heated at 65 °C for 1 h to obtain a bright red solution. Next, the solvent was removed in vacuo and the residue was washed with Et_2O to obtain a red solid. The solid was finally recrystallized from a CH_2Cl_2/toluene mixture. Yield: 220 mg (57%). X-ray quality crystals of dark red plates were grown via diffusion of Et_2O into a MeCN solution of the complex. Anal. Calcd for $C_{25}H_{26}ClN_6O_2Ru$ (**5**·MeCN): C, 51.86; H, 4.53; N, 14.51; Found: C, 52.08, H, 4.46; N, 14.31. Selected IR frequencies (KBr disk, cm^{-1}): 1597 (vs, ν_{CO}), 1478 (m), 1439 (m), 1331(m), 1299 (w), 1111 (w), 1029 (w), 768 (m), 684 (w). Electronic spectrum in MeCN, λ_{max} in nm (ϵ in M^{-1} cm^{-1}): 252 (25 190), 310 (10 170), 366 (15 050), 420 sh (6990), 508 (7120). X-band EPR spectrum in MeCN/toluene glass (*g*-values): 2.25, 2.20, 2.08, 1.91.

Physical Measurements. The ^1H NMR spectra were recorded at 298 K on a Varian 500 MHz instrument. A Perkin-Elmer Spectrum-One FT-IR spectrometer was used to monitor the IR spectra of the complexes. The electronic spectra were obtained with a scanning Carey 50 spectrophotometer (Varian). X-band EPR spectra were recorded using a Bruker 500 ELEXSYS spectrometer at 125 K. Release of NO in solution upon illumination was monitored with an *in*NO Nitric Oxide Measuring System (Innovative Instruments, Inc.) using the *ami*NO-2000 electrode. Electrochemical measurements were performed with standard Princeton Applied Research instrumentation and a Pt-inlay electrode. Half-wave potentials ($E_{1/2}$) were measured versus aqueous saturated calomel electrode (SCE).

Photolysis Experiments. The rates of NO release upon exposure to UV light were measured with ~0.1 mM solutions of the complexes in a 1 cm × 1 cm quartz cuvettes. The light source was an UV Transilluminator (UVP, Inc.) with peak intensity of 7 mW/cm^2 at 302 nm. At this wavelength, the 0.1 mM solutions of all three nitrosyls (**2**−**4**) absorbed all the light (absorbance values over 2). The cuvettes (placed at a distance of 3 cm) were exposed to UV light for no more than 40 s at a time to prevent thermal heating of the solution, and the electronic spectra were recorded at suitable time intervals. Quantum yield (ϕ) measurements were performed by using solutions of complexes in MeCN or H_2O in order to ensure sufficient absorbance (≥99%) at the incident wavelength; no more than 20% photolysis occurred in each measurement. Standard actinometry was performed with ferrioxalate[20a] and actinochrome N[20b] for the UV and visible regions, respectively. For EPR experiments, ~0.3 mM solutions of the complexes in MeCN were photolyzed exhaustively in quartz cuvettes. The samples were then transferred to EPR sample tubes, cooled, and their spectra recorded.

X-ray Crystallography. Diffraction data for **1**−**6** were collected at 90 K on a Bruker SMART 1000 (for **2**, **5**, and **6**) or a Bruker ApexII (for **1**, **3**, and **4**) instrument using Mo Kα radiation (λ = 0.71073 Å), and the data were corrected for absorption. The structures were solved using the standard SHELXS-97 package. The structure of **3** was refined as a pseudo-merohedral twin. Additional refinement details are contained in the CIF files (Supporting Information). Instrument parameters, crystal data, and data collection parameters for all the complexes are summarized in Table 1. Selected bond distances and bond angles for **1**−**4** are listed in Table 2, while those of **5**−**6** are listed in Table 3.

Results and Discussion

Synthesis of Ru−NO Complexes. Previously, we reported the syntheses of a number of {RuNO}^{6} nitrosyls starting from ruthenium(III) salts.[19,21] In the present work, reaction of $SBPy_3$ with $RuCl_3 \cdot 3H_2O$ in refluxing ethanol, however, led to hydrolysis of the *imine* function of the ligand to *amide* and only the Ru(III) complex **6** was isolated from the reaction mixture. This is unlike the reactions of $SBPy_3$ with Fe(III) salts in which the Fe(III) complex [$(SBPy_3)Fe(DMF)](ClO_4)_3$ is readily isolated at room temperature.[22] This is somewhat expected since the iron reaction is performed under very mild conditions and the desired Fe(III) complex is immediately precipitated out of the reaction mixture. Since $RuCl_3 \cdot 3H_2O$ does not react with $SBPy_3$ at room temperature, we decided to synthesize the desired nitrosyl complex **1** via use of Ru(II) starting materials. In general, ruthenium nitrosyls can be prepared by reacting Ru(II) precursors with nitrite salts under acidic conditions (eq 1). For example, Meyer[31] and others[14,32] have used this method to synthesize a wide variety of {RuNO}^{6} complexes, such as $[(bpy)_2Ru(NO)X]^{n+}$ ($X = Cl^-$ ($n = 2$); X = py, ($n = 3$)), [(terpy)(bpy)Ru(NO)]$^{3+}$, [Ru(NCS)(NO)(bpy)(py)]$^{2+}$, and $[Ru(NH_3)_4(NO)(isn)]$ (isn = isonicotinamide). In our work, reaction of $[Ru(DMSO)_4Cl_2]$ with $SBPy_3$ and $NaNO_2$/acid in

$$Ru^{II} - NO_2 + 2H^+ \rightarrow \{RuNO\}^6 + H_2O \qquad (1)$$

refluxing ethanol also afforded the desired nitrosyl complex **1**. Interestingly, replacement of $[Ru(DMSO)_4Cl_2]$ with $[Ru(MeCN)_4Cl_2]$ resulted in mixtures of **1** and the oxidized Ru(III) species **6**. It is therefore evident that the more stable $[Ru(DMSO)_4Cl_2]$ is a better starting material for the synthesis of **1**.

Although **2** was originally synthesized via direct replacement of the chloride ligand of **6** with NO in hot MeOH solution,[19] we have now discovered that treatment of **6** with

(31) (a) Godwin, J. B.; Meyer, T. J. *Inorg. Chem.* **1971**, *10*, 471. (b) Callahan, R. W.; Meyer, T. J. *Inorg. Chem.* **1977**, *16*, 574. (c) Pipes, D. W.; Meyer, T. J. *Inorg. Chem.* **1984**, *23*, 2466.
(32) (a) Nagao, H.; Ooyama, D.; Hirano, T.; Naoi, H.; Shimada, M.; Sasaki, S.; Nagao, N.; Mukaida, M.; Oi, T. *Inorg. Chim. Acta* **2001**, *320*, 60. (b) Sauaia, M. G.; da Silva, R. S. *Trans. Met. Chem.* **2003**, *28*, 254.

Table 1. Summary of Crystal Data and Intensity Collection and Structural Refinement Parameters for $[(SBPy_3)Ru(NO)](BF_4)_3$ (**1**), $[(PaPy_3)Ru(NO)](BF_4)_2$ (**2**·CH_3CN·$0.25Et_2O$), $[(Py_3P)Ru(NO)]BF_4$ (**3**), $[(Py_3P)Ru(NO)(Cl)]$ (**4**), $[(Py_3P)Ru(Cl)]$ (**5**·CH_3CN), and $[(PaPy_3)Ru(Cl)]BF_4$ (**6**·H_2O)

	1	**2**	**3**	**4**	**5**	**6**
empirical formula	$C_{20}H_{21}B_3F_{12}N_6ORu$	$C_{23}H_{25.50}B_2F_8N_7O_{2.25}Ru$	$C_{21}H_{19}BF_4N_6O_3Ru$	$C_{21}H_{19}ClN_6O_3Ru$	$C_{23}H_{22}ClN_6O_2Ru$	$C_{20}H_{22}BClF_4N_5O_2Ru$
fw	722.93	710.69	591.30	539.94	550.99	587.76
cryst color and habit	orange flat needle	yellow-orange dichroic needle	red needle	red plate	dark red plate	red plate
T	90(2) K	90(2) K	90(2) K	90(2) K	90(2) K	90(2) K
cryst syst	monoclinic	triclinic	triclinic	orthorhombic	monoclinic	monoclinic
space group	$C2/c$	$P\bar{1}$	$P\bar{1}$	$Pca2_1$	$P2_1/c$	$P2_1/c$
a, Å	21.468(5)	10.1081(12)	13.7575(9)	14.6611(5)	10.1334(12)	8.5012(11)
b, Å	9.254(2)	16.5739(18)	13.7599(9)	10.4632(4)	12.7761(15)	18.408(2)
c, Å	27.056(7)	17.3238(19)	14.8939(9)	13.3745(5)	17.245(2)	14.3838(17)
α, deg	90	75.761(4)	62.793(5)	90	90	90
β, deg	99.517(4)	86.966(4)	62.810(5)	90	94.899(5)	95.476(6)
γ, deg	90	84.073(7)	83.886(5)	90	90	90
V, Å^3	5301(2)	2796.9(5)	2211.6(2)	2051.68(13)	2224.5(5)	2240.7(5)
Z	8	4	4	4	4	4
d_{calcd}, Mg/m^3	1.812	1.688	1.776	1.748	1.645	1.742
abs coeff, μ, mm^{-1}	0.705	0.652	0.782	0.933	0.859	0.881
GOF on F^2	1.163	1.038	0.905	1.024	1.081	1.093
final R indices	R1 = 0.0779	R1 = 0.0470	R1 = 0.0348	R1 = 0.0174	R1 = 0.0279	R1 = 0.0251
[$I > 2\sigma(I)$]	wR2 = 0.2058	wR2 = 0.1029	wR2 = 0.0651	wR2 = 0.0460	wR2 = 0.0687	wR2 = 0.0579
R indices	R1 = 0.0939	R1 = 0.0692	R1 = 0.0428	R1 = 0.0177	R1 = 0.0375	R1 = 0.0283
(all data)	wR2 = 0.2183	wR2 = 0.1116	wR2 = 0.0676	wR2 = 0.0462	wR2 = 0.0759	wR2 = 0.0597

Table 2. Selected Bond Lengths (Å) and Bond Angles (deg) for $\{RuNO\}^6$ Complexes $[(SBPy_3)Ru(NO)](BF_4)_3$ (**1**), $[(PaPy_3)Ru(NO)](BF_4)_2$ (**2**·CH_3CN·$0.25Et_2O$), $[(Py_3P)Ru(NO)]BF_4$ (**3**), and $[(Py_3P)Ru(NO)(Cl)]$ (**4**)

	1	**2**	**3**	**4**
Ru−N(6)	1.773(7)	1.779(2)	1.746(3)	1.7583(12)
N(6)−O	1.129(9)	1.142(3)	1.154(4)	1.1390(16)
Ru−N(1)	2.105(7)	2.097(2)	2.173(3)	2.1128(12)
Ru−N(2)	2.010(7)	1.997(2)	2.098(3)	2.0407(11)
Ru−N(3)	2.085(6)	2.073(3)	2.001(4)	1.9851(11)
Ru−N(4)	2.054(7)	2.074(2)	2.024(3)	2.1110(10)
Ru−N(5)	2.098(6)	2.086(2)	2.122(3)	−
Ru−Cl(1)	−	−	−	2.3542(4)
N(2)−C(6)	1.286(11)	1.340(4)	−	−
N(2)−C(8)	−	−	1.361(5)	1.3414(17)
N(4)−C(14)	−	−	1.347(5)	1.3447(17)
C(6)−O(1)	−	1.230(4)	−	−
C(8)−O(1)	−	−	1.243(5)	1.2423(17)
C(14)−O(2)	−	−	1.247(5)	1.2428(18)
Ru−N(6)−O	175.5(7)	170.9(2)	172.0(3)	178.24(11)
N(6)−Ru−N(1)	98.6(3)	98.63(10)	170.39(14)	91.70(5)
N(6)−Ru−N(2)	173.8(3)	172.23(11)	92.98(14)	94.43(5)
N(6)−Ru−N(3)	92.7(3)	101.97(10)	94.81(14)	95.26(5)
N(6)−Ru−N(4)	101.4(3)	89.91(10)	99.43(14)	91.07(6)
N(6)−Ru−N(5)	94.8(3)	94.06(10)	89.14(13)	−
N(6)−Ru−Cl(1)	−	−	−	176.97(4)

Table 3. Selected Bond Lengths (Å) and Bond Angles (deg) for the Ru(III)−Cl Species $[(Py_3P)Ru(Cl)]$ (**5**·CH_3CN) and $[(PaPy_3)Ru(Cl)]BF_4$ (**6**·H_2O)[a]

	5	**6**
Ru−Cl(1)	2.3484(5)	2.4139(4)
Ru−N(1)	2.1285(15)	2.0917(14)
Ru−N(2)	2.0461(15)	1.9306(13)
Ru−N(3)	1.9634(15)	2.0689(13)
Ru−N(4)	2.0079(15)	2.0627(14)
Ru−N(5)	2.1054(15)	2.0725(14)
$N(2)-C(6)_{amide}$	−	1.354(2)
C(6)−O(1)	−	1.230(2)
$N(2)-C(8)_{amide}$	1.367(2)	−
$N(4)-C(14)_{amide}$	1.361(2)	−
C(8)−O(1)	1.238(2)	−
C(14)−O(2)	1.238(2)	−
Cl(1)−Ru−N(1)	175.20(4)	99.03(4)
Cl(1)−Ru−N(2)	94.90(5)	177.03(4)
Cl(1)−Ru−N(3)	88.32(4)	96.43(4)
Cl(1)−Ru−N(4)	91.75(5)	88.37(4)
Cl(1)−Ru−N(5)	86.00(4)	87.85(4)

[a] An ORTEP diagram (with numbering scheme) of **6** is provided in the Supporting Information (Figure S9).

$AgBF_4$ prior to exposure to NO gas (method A above) improves the yield of the desired nitrosyl **2**. This nitrosyl has also been synthesized by the reaction of the Ru(II) starting salt $[Ru(DMSO)_4Cl_2]$ with $PaPy_3^-$ in hot EtOH in presence of $NaNO_2$/acid (method B above). This one-step synthesis of **2** parallels the synthesis of **1** and affords **2** in higher yield.

Reaction of the Ru(III) "green solution" (prepared from $RuCl_3$·$3H_2O$ and hot ethanol) with the deprotonated dicarboxamide ligand Py_3P^{2-} in DMF cleanly affords the Ru(III) chloro species **5**. However, conversion of **5** to the corresponding nitrosyl **3** is not as straightforward. Exposure of **5** to NO gas in refluxing MeOH, EtOH, or hot DMF does not promote significant extent of NO binding. Addition of $AgBF_4$ in alcohols or H_2O/acetone mixtures[33] to assist the removal of Cl^- (and binding of NO) also proved ineffective in our hand. We suspect that the high affinity of the Ru^{III} center for Cl^- in $[(Py_3P)Ru(Cl)]$ (see structural parameters in Table 3) deters binding of NO in these reactions. The success in the syntheses of **1** and **2** using nitrite under acidic conditions and the difficulty encountered in direct binding of NO to **5** prompted us to pursue an analogous approach in case of **3**. Interestingly, reaction of $[Ru(MeCN)_4Cl_2]$ with Py_3P^{2-} in hot EtOH in presence of $NaNO_2$/acid afforded the orange complex **4**, in which one of the pyridine nitrogens of the ligand is not bound; instead a chloride ion is still bound to the metal center in a position trans to NO. Removal of the final chloride ion from **4** is, however, possible. Brief warming

(33) (a) Takeuchi, K.; Thompson, M. S.; Pipes, D. W.; Meyer, T. J. *Inorg. Chem.* **1984**, *23*, 1845. (b) Leising, R. A.; Ohman, J. S.; Takeuchi, K. J. *Inorg. Chem.* **1988**, *27*, 3804.

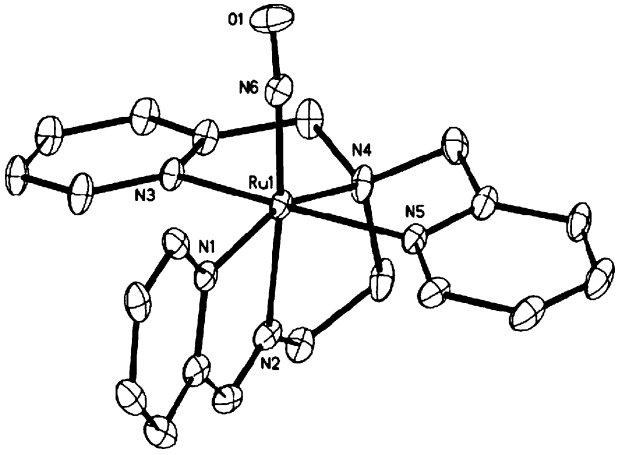

Figure 1. Thermal ellipsoid (probability level 50%) plot of $[(SBPy_3)Ru(NO)]^{3+}$ (the cation of **1**) with the atom labeling scheme. Hydrogen atoms have been omitted for the sake of clarity.

Scheme 1

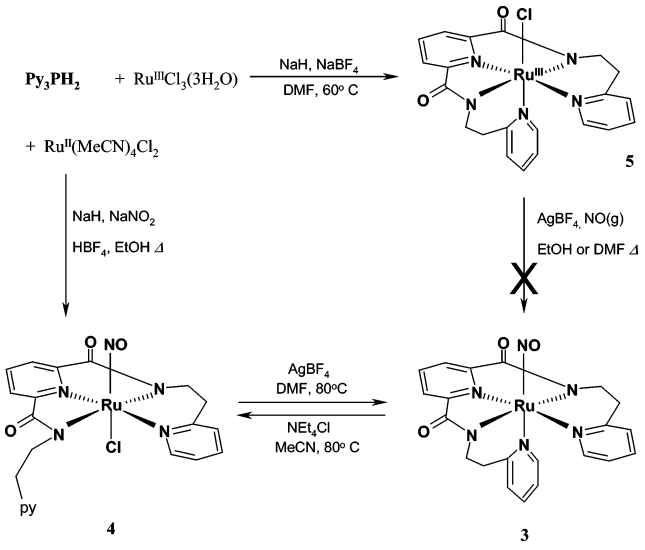

of a solution of **4** in DMF with $AgBF_4$ allows replacement of the chloride by the pyridine nitrogen of the dangling arm of the ligand. This final step affords the desired complex **3**, where the Py_3P^{2-} ligand is fully bound. Finally, while complex **3** is stable in solution over the course of several hours, the axial pyridine ligand is thermally labile to some extent, particularly in presence of chloride. When a solution of **3** in MeCN is heated for 1 h in the presence of a chloride source such as NEt_4Cl, the axial pyridine is replaced by chloride and complex **4** is obtained in almost quantitative yield. The reactions are summarized in Scheme 1 above.

Structures of the Complexes. $[(SBPy_3)Ru(NO)](BF_4)_3$ (1). The structure of the cation of **1** is shown in Figure 1, and selected structural parameters are listed in Table 1. The ruthenium center resides in a slightly distorted octahedral geometry similar to that observed in the corresponding iron[22] and manganese[25a] complexes. The imine N is trans to NO, while the remaining N donors coordinate in the equatorial plane. In **1**, the Ru−N(py) bond distances lie in a narrow range from 2.085(6) to 2.105(7) Å and are slightly longer than the Ru−N(4) (tertiary amine) bond of 2.054(7) Å.

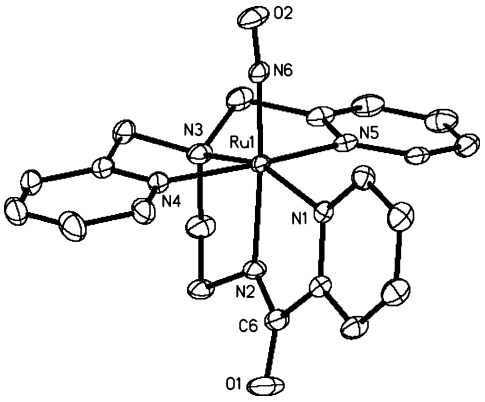

Figure 2. Thermal ellipsoid (probability level 50%) plot of $[(PaPy_3)Ru(NO)]^{2+}$ (the cation of **2**) with the atom labeling scheme. Hydrogen atoms have been omitted for the sake of clarity.

$[(PaPy_3)Ru(NO)](BF_4)_2 \cdot MeCN \cdot 1/4Et_2O$ ($2 \cdot MeCN \cdot 1/4Et_2O$). The structure of the cation of **2** is shown in Figure 2. Both the overall structure and the mode of coordination of the $PaPy_3^-$ ligand in **2** are very similar to those observed in other metal nitrosyls derived from this ligand.[24,25] In **2**, the carboxamido N donor is trans to NO and the ruthenium−carboxamido N bond length (Ru−N(2) = 1.997(2) Å) is slightly shorter than the corresponding Ru−N(imine) bond of **1** (2.010(7) Å). This shortening most possibly arises from the greater σ-donor strength of the negatively charged carboxamido nitrogen. The equatorial Ru−N(py) bond distances lie in a narrow range of 2.074(2)−2.097(2) Å and are similar to the Ru−N(py) bond lengths of **1** (Table 1).

Since complexes **1** and **2** are nearly isostructural, a comparison of the metric parameters of the $N_{imine/amido}$−Ru−NO vector provides some insight into imine N versus carboxamido N ligation in these two $\{RuNO\}^6$ nitrosyls. The nitrosyl N−O bond length of **1** (1.129(9) Å) is very close to that noted for other $\{RuNO\}^6$ nitrosyls derived from neutral polypyridine ligands such as $[Ru(terpy)(dpy)(NO)]^{3+}$ (dpy = 2,2′-dipyridylamine) (1.126(14) Å) or $[Ru(terpy)(dpk)(NO)]^{3+}$ (dpk = dipyridyl ketone) (1.126(8) Å).[34] The N−O bond of **2** is comparatively longer (1.142(3) Å). Similar N−O bond distances have been observed with $\{RuNO\}^6$ nitrosyls that contain negatively charged ligands, as in $[(^tBu_2Salophen)Ru(NO)(Cl)]$ (1.135(2) Å)[18] and [(bpb)Ru(NO)(Cl)] (1.1444(19) Å).[21] Interestingly, the Ru−N−O bond angles in **1** and **2** also reflect some differences. The Ru−NO unit in **1** is nearly linear at 175.5(7)°, while that of **2** is in a more bent configuration (170.9(2)°). Overall, the *longer* N−O bond and more *bent* Ru−N−O angle observed in **2** versus **1** is consistent with the carboxamido N facilitating greater transfer of electron density to the π^* orbital of NO from the metal center.

$[(Py_3P)Ru(NO)]BF_4$. The structure of the cation of **3** (Figure 3) reveals that the deprotonated Py_3P^{2-} ligand is fully bound to the $\{RuNO\}^6$ core in a slightly distorted octahedral fashion. Two carboxamido nitrogens of this ligand coordinate in the equatorial plane, trans to one another. The rest of the

(34) (a) Chanda, N.; Mobin, S. M.; Puranik, V. G.; Datta, A.; Niemeyer, M.; Lahiri, G. K. *Inorg. Chem.* **2004**, *43*, 1056. (b) Sarkar, S.; Sarkar, B.; Chanda, N.; Kar, S.; Mobin, S. M.; Fiedler, J.; Kaim, W.; Lahiri, G. K. *Inorg. Chem.* **2005**, *44*, 6092.

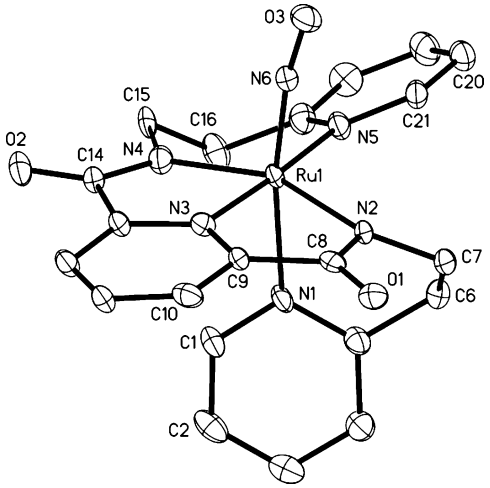

Figure 3. Thermal ellipsoid (probability level 50%) plot of $[(Py_3P)Ru(NO)]^+$ (the cation of **3**) with the atom labeling scheme. Hydrogen atoms have been omitted for the sake of clarity.

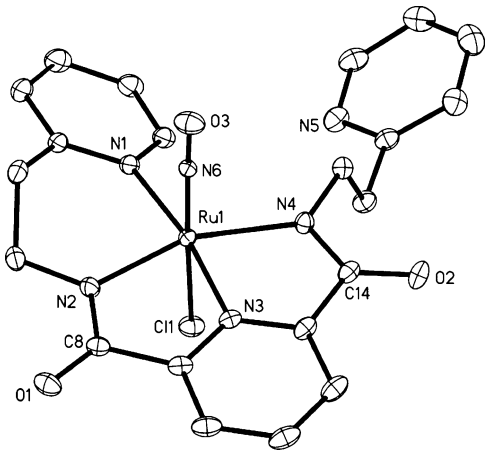

Figure 4. Thermal ellipsoid (probability level 50%) plot of $[(Py_3P)Ru(NO)(Cl)]$ (**4**) with the atom labeling scheme. Hydrogen atoms have been omitted for the sake of clarity.

equatorial coordination is completed by two pyridine nitrogens, and the remaining pyridine binds the axial position trans to NO. A similar mode of Py_3P^{2-} binding has been observed in several octahedral cobalt complexes.[27]

The ruthenium−carboxamido N bond lengths (Ru−N(2) = 2.098(3) and Ru−N(4) = 2.034(4) Å) of **3** are longer than the same distance in **2** (Ru−N(2) = 1.997(2) Å). Compared to the equatorial Ru−N5(py) bond (2.128(3) Å), the axial Ru−N1(py) bond of **3** is longer (2.148(3) Å) due the trans effect of the NO ligand. The Ru−N(O) bond of **3** (1.751(3) Å) is also noticeably shorter than the Ru−N(O) bond of **2** (1.779(2) Å). We ascribe this shortening due to the weaker trans effect of pyridine (in **3**) compared to carboxamido nitrogen (a stronger σ-donor) in **2**. The Ru−N−O angles of **2** (170.9(2)°) and **3** (172.0(3)°) are, however, very close to each other.

$[(Py_3P)Ru(NO)(Cl)]$ (4). The structure of **4** (Figure 4) reveals that the Py_3P^{2-} ligand is partially bound to the $\{RuNO\}^6$ unit in this nitrosyl. When compared to the structure of **3** (Figure 3), it is evident that the axial pyridine nitrogen of the ligand is *not bound* to the ruthenium in **4**. Instead, a chloride ion occupies the axial position trans to

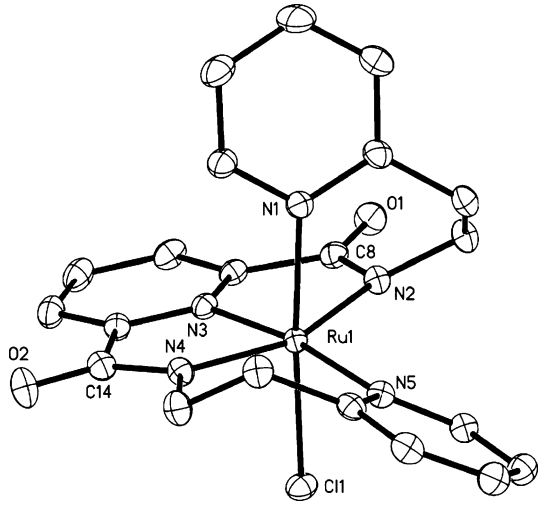

Figure 5. Thermal ellipsoid (probability level 50%) plot of $[(Py_3P)Ru(Cl)]$ (**5**) with the atom labeling scheme. Hydrogen atoms have been omitted for the sake of clarity.

NO. There is precedence of partial coordination of the Py_3P^{2-} ligand to the metal center. For example, we have reported an Fe(III) complex of Py_3P^{2-} ligand, namely, $Na[(Py_3P)_2Fe]$, in which both pyridine arms of each Py_3P^{2-} ligand are not bound to the iron center.[28]

$[(Py_3P)Ru(Cl)]\cdot MeCN$ (5·MeCN). The structure of the Ru(III)−chloro complex **5** is shown in Figure 5. In this complex, the Py_3P^{2-} ligand is properly bound, much like in **3**. Complex **5** exhibits one interesting structural difference compared to the $\{RuNO\}^6$ nitrosyl **3** (Tables 1 and 2). All the ruthenium−nitrogen distances of **5** are slightly shorter, a fact consistent with the presence of an authentic Ru(III) center in this complex.

When one compares the structural parameters of **5** with those of the Ru(III)−chloro species derived from $PaPy_3^-$ ligand, namely, **6** (Table 2), an interesting structural feature emerges. The Ru(III)−Cl bond of **5** (2.3484(5) Å) is significantly shorter than that of **6** (2.4139(4) Å). This lengthening of the Ru(III)−Cl bond in **6** most possibly arises from the trans effect of the carboxamido nitrogen (a stronger donor compared to pyridine). As a consequence, NO readily replaces Cl^- from **6** (affording **2**) but *not* from **5** under any conditions.

Spectroscopic Properties. Binding of the carboxamido N(s) of the two ligands to the ruthenium centers in **2**−**6** is evident by the shift of the carbonyl stretch (ν_{CO}) to lower frequency.[21−25,27,35] For example, **2** exhibits its ν_{CO} at 1634 cm^{-1} as compared to the ν_{CO} of free $PaPy_3H$, 1666 cm^{-1}. Similarly, **3** displays its ν_{CO} at 1611 cm^{-1} (for free Py_3PH_2, ν_{CO} = 1654 cm^{-1}). The NO stretching frequency (ν_{NO}) of the four nitrosyl complexes **1**−**4** follows an interesting trend. Although the N−O bond distances of **1**−**4** lie in a narrow range of 1.12−1.15 Å, the ν_{NO} values clearly show differences indicating changes in N−O bond strength (Figure 6). Complex **1** exhibits its ν_{NO} at 1920 cm^{-1}, similar to other nitrosyls derived from neutral polypyridine ligands such as $[Ru(NO)(MeCN)(bpy)_2]^{3+}$ (1924 cm^{-1}).[32a] The ν_{NO} stretch

(35) Marlin, D. S.; Mascharak, P. K. *Chem. Soc. Rev.* **2000**, *29*, 69.

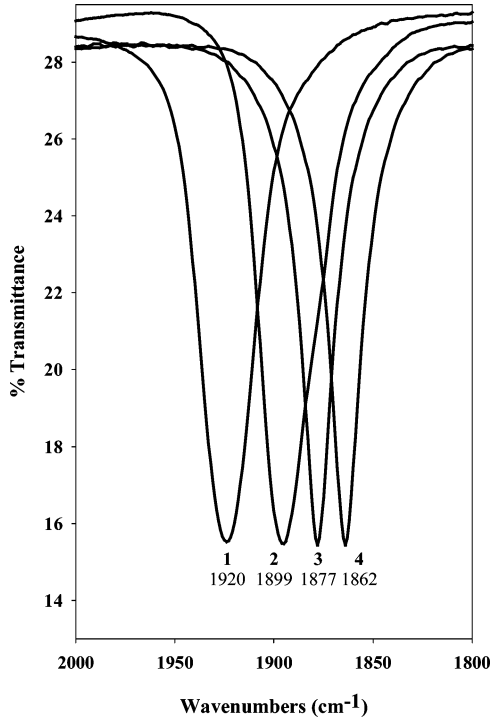

Figure 6. NO stretching frequency (ν_{NO}) of nitrosyl complexes **1**−**4** in KBr pellet.

in **2** appears at 1899 cm^{-1}, a value in good agreement with other nitrosyls that contain negatively charged ligands such as $[Ru(NO)(tpy)(Cl)_2]$ (1895 cm^{-1}).[36] The effect of an additional carboxamido N donor is evident in the IR spectrum of **3**; the ν(NO) stretch of **3** is shifted to lower frequency by another 20 cm^{-1} to 1877 cm^{-1}. Overall, there is a clear trend of decreasing ν_{NO} (N−O bond strength) in the order **1** (1920 cm^{-1}) > **2** (1899 cm^{-1}) > **3** (1877 cm^{-1}) as the number of carboxamido N increases from zero (in **1**) to one (in **2**) to two (in **3**). This trend closely parallels the N−O bond distance order **1** (1.129(9) Å) < **2** (1.142(3) Å) < **3** (1.154(4) Å). Clearly, electron donation to the ruthenium center by the increasing number of negatively charged carboxamido N(s) facilitates greater transfer of electron density to the π^* orbital of NO and results in this trend of weakening of the N−O bond in these three nitrosyls. The presence of chloride ion in **4** lowers the value of ν_{NO} further to 1862 cm^{-1} (Figure 6) due to the greater σ-donor strength of Cl^- (in **4**) versus pyridine N (in **3**).

All four $\{RuNO\}^6$ nitrosyls (**1**−**4**) are diamagnetic and exhibit sharp peaks in their NMR spectra at 298 K (for ^1H NMR spectra of **1**−**4**, see Supporting Information, Figures S1−S4). As expected, the Ru(III)−Cl complexes **5** and **6** are paramagnetic and exhibit *g*-values consistent with their low-spin d^5 configuration (see Experimental Section and ref 19).

Electronic Absorption Spectra. Complex **1** exhibits an intense absorption band centered at 315 nm much like other $\{RuNO\}^6$ species derived from neutral polypyridine ligands such as $[Ru(NO)(bpy)_2(py)]^{3+}$ (325 nm) and $[Ru(NO)(trpy)(bpy)]^{3+}$ (336 nm). Such bands have previously been assigned as metal-to-ligand charge transfer (MLCT) involving a d(Ru)→π^*(NO) transition. This transition has been proposed to be responsible for the photolability of the $\{RuNO\}^6$ moiety.[31] Complex **2** exhibits its absorption band at 410 nm. This charge-transfer (CT) band is red-shifted ∼100 nm compared to the CT band for **1**. In general, $\{RuNO\}^6$ complexes derived from charged ligands such as [(salen)Ru(NO)(Cl)] (λ_{max} = 376 nm)[18] and $[(Me_2bpb)Ru(NO)(Cl)]$ (λ_{max} = 395 nm)[21] also display their CT band in the region of 400 nm. This red-shift of the CT band arises from coordination of the negatively charged donor atoms that increase electron density at the metal center and facilitate d(Ru)→π^*(NO) transition at a lower energy.[18] Complex **3** dissolves in MeCN to afford a *red* solution that exhibits additional absorption near 530 nm. Complex **4** also exhibits a similar feature in this region (520 nm).

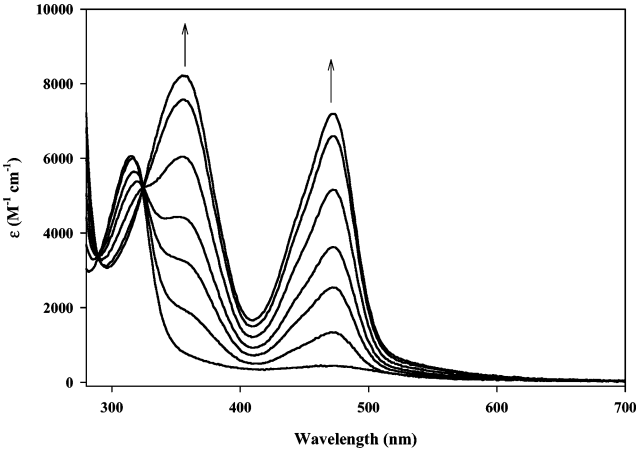

Figure 7. Changes observed in electronic spectrum of **1** (MeCN, 0.1 mM) upon exposure to low-intensity UV light at ∼15 s intervals.

Photolability of the Nitrosyls. Complex 1. Complex **1** is indefinitely stable in MeCN in the dark or under ambient light conditions. However, exposure of such solution to low-intensity UV light ($\lambda_{irr} \approx$ 300 nm) causes a distinctive color change from light yellow to a deep orange. Isosbestic points (at 320 and 290 nm) noted in the absorption spectra of the solution undergoing photolysis (Figure 7) confirm clean conversion of **1** to its photoproduct (vide infra). In addition, two new absorption bands are generated at 355 and 470 nm. Complex **1** is also soluble in water, and similar changes in the electronic spectrum are observed upon UV photolysis. However, caution must be taken as dissolution of **1** in water (pH ∼7) leads to partial decomposition, most likely due to NO→NO_2 conversion, as noted in many other cases.[32,33,37] Such decomposition can be avoided by performing the photolysis under acidic conditions (pH 3, phosphate buffer). The instability of **1** at physiological pH is a notable disadvantage that severely limits its use as an NO donor in biological systems. We have confirmed the release of NO from **1** upon UV illumination with the use of NO electrode

(36) Hirano, T.; Ueda, K.; Mukaida, M.; Nagao, H.; Oi, T. *J. Chem. Soc. Dalton Trans.* **2001**, 2341.

(37) (a) Byabartta, P.; Jasimuddin, S.; Ghosh, B. K.; Sinha, C.; Slawin, A. M. Z.; Woollins, J. D. *New J. Chem.* **2002**, *26*, 1415. (b) Freedman, D. A.; Janzen, D. E.; Vreeland, J. L.; Tully, H. M.; Mann, K. R. *Inorg. Chem.* **2002**, *41*, 3820.

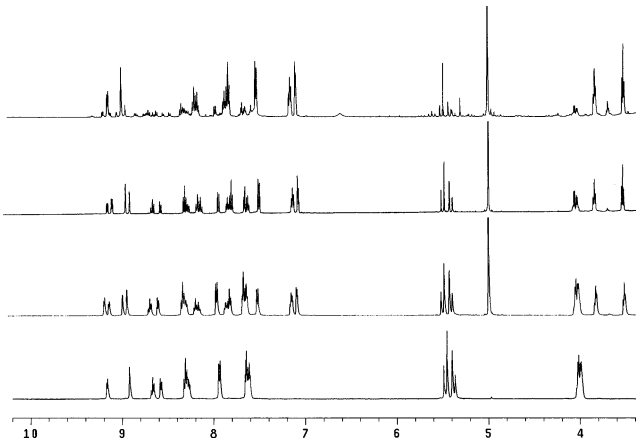

Figure 8. ^{1}H NMR spectra of **1** in CD_3CN during photolysis with low-intensity UV light at the indicated photolysis increments (500 MHz Bruker spectrometer, 298 K). From bottom to top: *no* photolysis, ~40% photolysis, ~60% photolysis, ~95% photolysis.

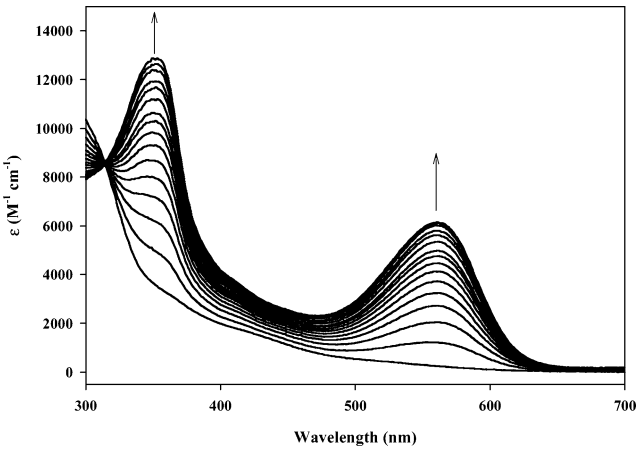

Figure 9. Changes in electronic absorption spectra of **3** in MeCN upon exposure to UV light. New peaks at 350 and 560 nm are generated along with an isosbestic point at 315 nm.

(Figure S5, Supporting Information). Such experiments nicely demonstrate that NO is released only upon exposure to UV light and the amount of photoreleased NO is proportional to the exposure time.

Photoproduct of 1. As shown in Figure 7, photolysis of **1** in MeCN generates two new, intense absorption bands at 355 and 470 nm. Interestingly, the final absorption spectrum of the photoproduct is very similar to that of the corresponding Fe(II)−solvato species $[(SBPy_3)Fe^{II}(MeCN)]^{2+}$ previously synthesized and structurally characterized by this group.[22] This iron−solvato species exhibits one intense absorption band at 355 nm (same as the photoproduct from **1**) and another at 570 nm. This latter band at 570 nm is a MLCT band of $[(SBPy_3)Fe^{II}(MeCN)]^{2+}$. Since one expects such MLCT band to blue-shift in case of Ru(II), it is apparent that the photoproduct of **1** is the Ru(II)−solvato species $[(SBPy_3)Ru^{II}(MeCN)]^{2+}$.

To confirm the oxidation state of ruthenium in the photoproduct, we have examined the EPR and ^{1}H NMR spectra of the photolyzed solutions. Photolysis of **1** in MeCN (or water) generates a solution that exhibits no EPR spectrum. When the photolysis (in CD_3CN or D_2O) is monitored by ^{1}H NMR spectroscopy, one observes clean conversion of **1** to a second *diamagnetic* species. As shown in Figure 8, the peaks at 4.0 and 5.4 ppm of **1** are gradually replaced by new peaks at 3.6, 3.8, and 5.0 ppm upon photolysis. Additional changes are also observed in the aromatic region. The final ^{1}H NMR spectrum is strikingly similar to that of $[(SBPy_3)Fe^{II}(MeCN)]^{2+}$. The photolyzed solution of **1** also exhibits a positive ion peak at $m/z = 236.64$ in its mass spectrum which corresponds to the expected value for $[(SBPy_3)Ru^{II}(MeCN)]^{2+}$ ($m = 473$, $z = 2+$). Finally, we have synthesized $[(SBPy_3)Ru^{II}(MeCN)]^{2+}$ via reductive de-nitrosylation of **1** with azide, a method frequently used to generate Ru(II)−solvato species from $\{RuNO\}^6$ nitrosyls.[38] Reductive de-nitrosylation of **1** in situ generates an electronic spectrum *identical* to that obtained upon photolysis of **1**.

Generation of $[(SBPy_3)Ru^{II}(MeCN)]^{2+}$ as the photoproduct of **1** is quite consistent with the known chemistry of $SBPy_3$. We have previously shown that this ligand stabilizes the +2 oxidation state of iron to a great extent.[22] For example, $[(SBPy_3)Fe^{II}(MeCN)]^{2+}$ is *spontaneously* (and rapidly) generated when $[(SBPy_3)Fe^{III}(DMF)]^{3+}$ is dissolved in MeCN. In the case of **1**, the photorelease of NO in MeCN therefore affords $[(SBPy_3)Ru^{II}(MeCN)]^{2+}$, the species containing ruthenium in the +2 oxidation state (also see electrochemistry).

Photolysis of 2−4. Previously, we have shown that exposure of an aqueous solution of **2** to low-intensity UV light (~5 mW) prompts rapid release of NO.[19] In such work, **2** was employed to deliver NO to biological targets such as myoglobin (Mb) and cytochrome *c* oxidase.[19,20a] NO photoreleased from **2** can be easily detected in such systems by the use of NO electrode (Figure S6, Supporting Information). In the present work, photorelease of NO from **2** has been studied in MeCN. When a solution of **2** in MeCN is exposed to low-intensity UV light ($\lambda_{max} = 305$ nm) for several minutes, new peaks are generated at 490 and 350 nm. A clean isosbestic point is observed at 320 nm (Figure S7, Supporting Information).

Complex **3** also exhibits NO photolability in MeCN. In this case, the orange-red solution of **3** turns dark violet within minutes of exposure to UV light. An intense absorption peak at 560 nm develops with time (Figure 9). Thus, the loss of NO can be conveniently monitored by changes in the electronic spectra of these nitrosyls.

Quantum Yields. The quantum yield (ϕ) values of **2**−**4** indicate the efficiency of NO release from these $\{M-NO\}^6$ nitrosyls. In the present work, we have measured the ϕ values of the nitrosyls by using a low-intensity UV light (see Experimental Section) with peak intensity of 7 mW/cm^2 at 302 nm. The ϕ values increase upon going from **2** ($\phi = 0.06 \pm 0.01$) to **3** ($\phi = 0.15 \pm 0.01$) to **4** ($\phi = 0.17 \pm 0.01$). The higher ϕ values observed for **3** and **4** compare favorably with ϕ values of other ruthenium NO donors such as $[Ru(NO)Cl_5]^{2-}$ ($\phi = 0.06$),[39] [Ru(salen)(Cl)(NO)] ($\phi = 0.13$),[18] and [Ru-

(38) (a) Cicogna, F.; Ingrosso, G.; Marcaccio, M.; Paolucci, D.; Paolucci, F.; Trillini, L. *J. Organomet. Chem.* **2006**, *691*, 1425. (b) Coe, B. J.; Meyer, T. J.; White, P. S. *Inorg. Chem.* **1995**, *34*, 593. (c) Sellmann, D.; Geck, M.; Moll, M. *Z. Naturforsch.* **1992**, *47b*, 74.

(39) Bettache, N.; Carter, T.; Corrie, G. E. T.; Ogden, D.; Trentham, D. R. *Methods Enzymol.* **1996**, *268*, 266.

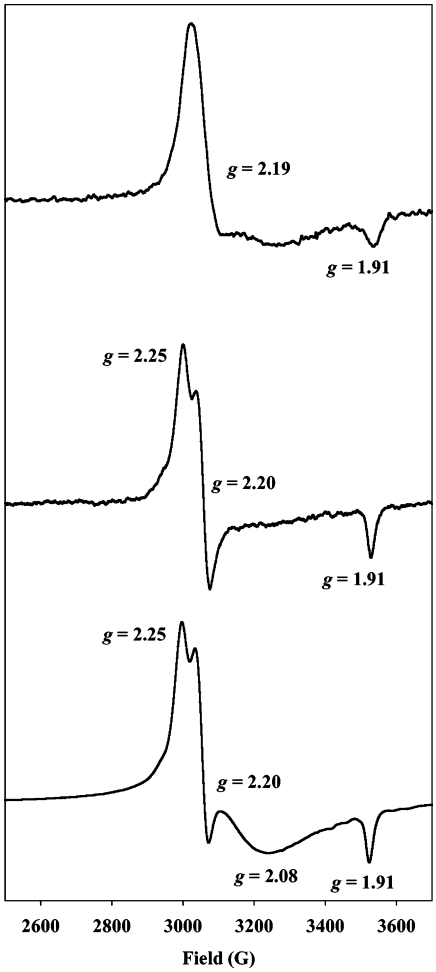

Figure 10. X-band EPR spectra in MeCN/toluene glass of photoproduct of **3** following UV photolysis (top); photoproduct of **4** after UV photolysis (middle); and authentic Ru(III) complex $[(Py_3P)Ru^{III}(Cl)]$ (**5**, bottom). Instrument parameters: temperature, 125 K; microwave power, 1 mW; microwave frequency, 9.4 GHz; frequency modulation, 100 kHz.

$(NH_3)_4(py)(NO)]$ ($\phi = 0.13$).[40] Since **3** is a more efficient NO donor than **2**, it is evident that increase in the number of carboxamido N's (from one in **2**, to two in **3**) accelerates the release of NO in these nitrosyls. The higher ϕ value of **4** indicates additional dependence of photolability of bound NO on structural features. Complex **4** contains a bound chloride ion (trans to NO) in addition to two carboxamido N's. The presence of the negatively charged chloride ligand trans to NO clearly enhances the NO photolability of this nitrosyl compared to **3** in which a neutral pyridine N occupies the same position. Previously, we[21] (and others[18]) have shown that charged axial ligands such as chloride increases photolability of ruthenium nitrosyls. In the present study, **4** exhibits the highest quantum efficiency compared to all other related ruthenium nitrosyls reported here (**1**−**3**) and in our previous reports.[19,21]

In order to determine the utility of these nitrosyls in photodynamic therapy (commonly utilizing visible light of higher wavelengths),[41] we have also checked the effect(s) of visible light on them. Both **1** and **2** exhibit little to no absorbance in the visible region (≥450 nm) and are thus responsive only to UV light. In contrast, **3** and **4** are somewhat sensitive to visible light. For example, exposure of solutions of **3** and **4** in MeCN to 532 nm light source (Nd:YAG laser) leads to photorelease of NO as evidenced by rapid changes in color. The ϕ values of **3** and **4** at this wavelength are 0.050 ± 0.004 and 0.064 ± 0.003, respectively. Interestingly, similar behavior has been noted with $[Ru(NO)(py^{bu}S_4)]Br$ and $[Ru(NO)(py^{si}S_4)]Br$, which also contain two negatively charged donors (thiolato S) in the ligand system.[42] Clearly, the two carboxamido N donors in **3** and **4** sensitize the $\{RuNO\}^6$ moiety to visible light much like the two thiolato S donors in the latter compounds.

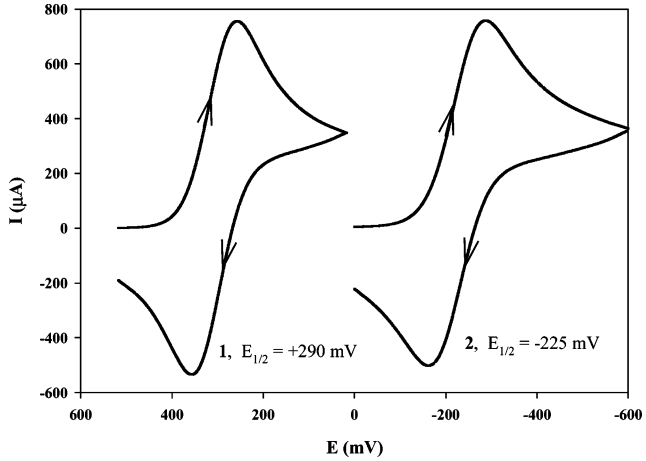

Figure 11. Cyclic voltammograms of **1** and **2** in MeCN (0.10 M NEt_4ClO_4, scan rate = 50 mV/s). Halfwave potentials ($E_{1/2}$) values are indicated vs aqueous SCE.

Photoproducts of 2−4. Quite contrary to **1**, photolyzed solutions of **2**−**4** are paramagnetic and display intense EPR signals. It is evident that in these cases, photolysis gives rise to Ru(III) species upon release of NO (eq 2). Photolysis of $\{RuNO\}^6$ complexes are known to generate paramagnetic Ru(III) photoproducts many of which have been identified by EPR spectroscopy.[13b,14,20a,21,43]

$$\{RuNO\}^6 + h\nu \rightarrow Ru^{III} - (solv) + NO \qquad (2)$$

The EPR spectrum of **2** following photolysis in MeCN confirms the presence of a low-spin, d^5 Ru(III) species. The overall slightly asymmetric axial spectrum ($g = 2.22$, 2.20, and 1.91) is very similar to that $[(PaPy_3)Fe^{III}(MeCN)]^{2+}$ ($g = 2.36$, 2.21, 1.89),[23] a fact that confirms the presence of $[(PaPy_3)Ru^{III}(MeCN)]^{2+}$ as the photolyzed product. Photolysis of **3** in MeCN generates a strictly axial EPR signal with $g = 2.19$ and 1.91 while the photoproduct of **4** exhibits a slightly rhombic EPR signal that is similar to the spectrum of authentic Ru(III) species **5** (Figure 10).

(40) Tfouni, E.; Krieger, M.; McGarvey, B. R.; Franco, D. W. *Coord. Chem. Rev.* **2003**, *236*, 57.

(41) Pandey, R. K. *J. Porphyrins Phthalocyanines* **2000**, *4*, 368. (b) Ackroyd, R.; Kelty, C.; Brown, N.; Reed, M. *Photochem. Photobiol.* **2001**, *74*, 656. (c) Detty, M. R.; Gibson, S. L.; Wagner, S. J. *J. Med. Chem.* **2004**, *47*, 3897.

(42) Prakash, R.; Czaja, A. U.; Heinemann, F. W.; Sellmann, D. *J. Am. Chem. Soc.* **2005**, *127*, 13758.

(43) Komozin, P. N.; Kazakova, V. M.; Miroshnichenko, I. V.; Sinitsyn, N. M. *Russ. J. Inorg. Chem.* **1983**, *28*, 1806.

Electrochemistry. In MeCN, **1** exhibits a reversible voltammogram with $E_{1/2} = +0.290$ V (Figure 11). This $E_{1/2}$ value is close to that of other ruthenium nitrosyls derived from polypyridine ligands such as $[(trpy)(bpy)Ru(NO)]^{3+}$ (+0.45 V) and $[(bpy)_2Ru(NO)(MeCN)]^{3+}$ (+0.56 V). Complex **2** on the other hand exhibits a reversible voltammogram with a more negative $E_{1/2}$ value (−0.225 V). This difference arises from the nature of the two ligands. Since the neutral $SBPy_3$ ligand provides more stability to the +2 oxidation state of ruthenium, it facilitates reduction of the $\{RuNO\}^6$ moiety. In contrast, $PaPy_3^-$ is known to provide stability to +3 oxidation state in general and hence the $\{RuNO\}^6$ moiety in **2** is more resistant to reduction. The ligand Py_3P^{2-} also stabilizes +3 oxidation state, and hence, **3** exhibits a negative $E_{1/2}$ value (−0.205 V) in MeCN.

The redox potential values (Figure 11) explain why photolysis of **1** affords a Ru(II) species while photolysis of **2** and **3** results in Ru(III) products. It is quite possible that photolysis of the $\{RuNO\}^6$ nitrosyl **1** initially affords a Ru(III)−solvato species which is spontaneously reduced to $[(SBPy_3)Ru^{II}(MeCN)]^{2+}$ (much like its Fe(III) analogue[22]) in MeCN solution. As a result, only $[(SBPy_3)Ru^{II}(MeCN)]^{2+}$ is observed as the photoproduct of **1**. In case of **2** and **3**, the Ru(III)−solvato species are more stable, and hence, one obtains $[(PaPy_3)Ru^{III}(MeCN)]^{2+}$ and $[(Py_3P)Ru^{III}(MeCN)]^{+}$, respectively, as the sole photoproduct. This is further supported by the fact that $[(Me_2bpb)Ru(NO)(py)]BF_4$, a photolabile $\{RuNO\}^6$ nitrosyl with Me_2bpb^{2-} ligand (with two carboxamido N's in the equatorial plane), also exhibits a reversible cyclic voltammogram with $E_{1/2} = -0.270$ V and affords a Ru(III) photoproduct.[21,44]

Conclusions

The results of this work demonstrate that $\{RuNO\}^6$ nitrosyls derived from a set of analogous ligands with zero, one, and two built-in carboxamide groups all exhibit photolability upon exposure to low-intensity UV light. However, the efficiency of NO release increases as the number of carboxamide group(s) in the ligand increases. When such polypyridine ligand does not provide any carboxamido N donor to the ruthenium center, photorelease of NO results in Ru(II) photoproducts. In contrast, the presence of carboxamido N(s) in the coordination sphere of ruthenium in such nitrosyls affords Ru(III) photoproducts following photorelease of NO. Since complexes **2**−**4** exhibit excellent stability in aqueous media and moderately fast NO release upon illumination with low-intensity UV light, we are currently investigating their use in nitrosylation of biological targets. Results of such studies will be reported in due time.

Acknowledgment. This research was supported by a grant from the National Science Foundation (CHE-0553405). E.A.A. received financial support from NIH IMSD Grant No. GM58903. Experimental assistance from Dr. Jayashree Ray is gratefully acknowledged.

Supporting Information Available: ^{1}H NMR spectra of **1**−**4** (Figures S1−S4), NO amperograms for **1** and **2** in water (Figures S5, S6), changes in electronic absorption spectra of **2** and **4** in MeCN upon photolysis (Figures S7, S8), ORTEP diagram of **6** with numbering scheme (Figure S9), and X-ray crystallographic data (in CIF format) for **1**−**6**. This material is available free of charge via the Internet at http://pubs.acs.org.

IC0620945

(44) The photoproduct $[(Me_2bpb)Ru(py)(MeCN)]^+$ exhibits a strong EPR signal with $g = 2.17$ and 1.88 (see ref 21).